


Nuclear β spectrum from the projected shell model: Allowed one-to-one transition

Fan Gao, Zi-Rui Chen, and Long-Jun Wang 

School of Physical Science and Technology, Southwest University, Chongqing 400715, China



(Received 22 August 2023; accepted 9 November 2023; published 27 November 2023)

Nuclear β spectrum and the corresponding (anti)neutrino spectrum play important roles in many aspects of nuclear astrophysics, particle physics, nuclear industry, and nuclear data. In this work we propose a projected shell model (PSM) to calculate the level energies as well as the reduced one-body transition density (ROBTD) by the Pfaffian algorithm for nuclear β decays. The calculated level energies and ROBTD are inputted to the beta spectrum generator (BSG) code to study the high precision β spectrum of allowed one-to-one transitions. When experimental level energies are adopted, the calculated β spectrum by ROBTD of the PSM deviates from the one by the extreme simple particle evaluation of the BSG by up to 10%, reflecting the importance of nuclear many-body correlations. When calculated level energies are adopted, the calculated β spectrum shows sensitive dependence on the reliability of calculated level energies. The developed method for ROBTD by the PSM will also be useful for study of the first-forbidden transitions, the isovector spin monopole resonance, etc., in a straightforward way.

DOI: [10.1103/PhysRevC.108.054313](https://doi.org/10.1103/PhysRevC.108.054313)

I. INTRODUCTION

Nuclear β decay plays crucial roles in many frontiers in nuclear astrophysics and nuclear physics. For nuclear astrophysics, the understanding of many astrophysical problems such as the cooling of neutron stars [1,2], the origin of heavy elements by rapid neutron and proton capture processes, etc. [3–5], rely heavily on effective β -decay rates of finite nuclei in stellar environments with high temperature and high density.

The nuclear β spectrum, and the neutrino spectrum accordingly, i.e., the probability of the electron and antineutrino emission (positron and neutrino emission) as a function of the corresponding kinetic energy for β^- decay (β^+ decay), are important for nuclear astrophysics, particle physics, nuclear industry, and nuclear data [6–9]. The integrated form of the β spectrum turns out to be the most precise way to determine the up-down quark element of the Cabibbo-Kobayashi-Maskawa matrix V_{ud} [10]. The β spectrum is also needed in nuclear medicine for radiotherapy and dosimetry, and in the nuclear industry for calculations of residual power or post-irradiation fuel management [6,11]. The neutrino spectra of reactors provide one of the techniques for monitoring nuclear facilities, and the reactor antineutrino anomaly is still a puzzle to be solved for the community [12–27].

In practical investigations and applications, β spectra and neutrino spectra of many nuclei, including some exotic ones that cannot be touched experimentally so far, are indispensable so that both experimental measurements and theoretical calculations are expected. Accordingly, some aspects need to be noted for the study of nuclear β and neutrino spectra, following the schematic diagram of the β decay scheme as shown

in Fig. 1. (i) One-to-one transition spectrum and the total spectrum: As seen from Fig. 1, the initial state (usually the ground state while sometimes an isomer) of some parent nucleus can β decay to each state of the corresponding daughter nucleus within the Q_β value, where each one-to-one (individual) transition has the corresponding feeding intensity $I(\%)$ and comparative half-life $\log ft$. Each individual transition has corresponding one-to-one transition β spectrum and the total β spectrum can be obtained theoretically by summing over all related normalized one-to-one transition β spectrum weighted by corresponding $I(\%)$. This indicates that reliable calculation of the total β spectrum depends on reasonable description of both the one-to-one transition β spectra and the $I(\%)$. (ii) Allowed and forbidden transitions: Not only allowed but also forbidden transitions can provide sizable contributions to the total β spectrum. As seen from the schematic diagram in Fig. 1, the transition to the 1^+ state (2^- state) with excitation energy E_{f2} (E_{f1}) is allowed (first-forbidden), both transitions may have similar $\log ft$ and $I(\%)$ so that they may provide similar contribution to the total spectrum. Actually, there are many nuclei whose $I(\%)$ is dominated by a single forbidden transition (such as ^{92}Rb , ^{89}Sr , ^{96}Y , ^{137}Xe , ^{142}Cs , etc.), and thus the total spectrum is determined by reliable description of the forbidden transition theoretically. (iii) Contribution of highly excited states: Nuclear levels are usually discrete for low-lying states, and become denser and denser with excitation energy so that the level density $\rho(E)$ is large for highly excited states (especially of odd-mass and odd-odd nuclei). For β decay with large Q_β , the contribution from highly excited states with large $\rho(E)$ should also be considered accurately and precisely in the total β spectrum. Experimentally, the $I(\%)$ of highly excited states cannot be obtained accurately by the traditional method for γ -ray spectroscopy measurements with the high purity germanium (HPGe) arrays which have high energy resolution but low efficiency. This is referred to as

*longjun@swu.edu.cn

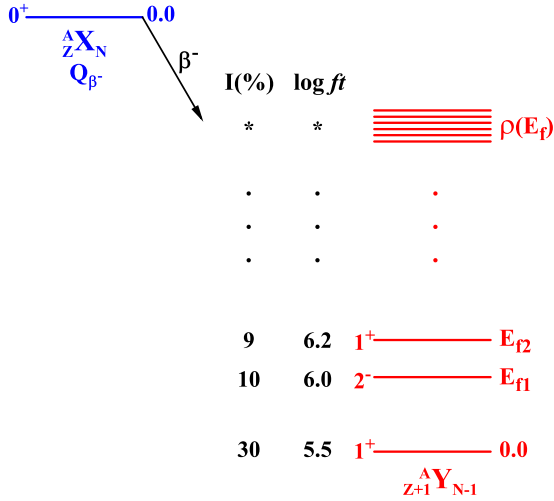


FIG. 1. A schematic diagram for the β decay scheme of some even-even nucleus AX .

the pandemonium effect [28]. The problem can be overcome by adopting inorganic scintillators such as NaI that have very high efficiency but reduced energy resolution, corresponding to the modern total absorption γ -ray spectroscopy (TAGS) technique [23,29]. Theoretically, large model space and configuration space are crucial for reliably modeling the $I(\%)$ of highly excited states.

It can then be seen that reliable calculation of the total β and neutrino spectra requires nuclear-structure models to treat reasonably both allowed and forbidden transitions, to have large model and configuration spaces for a description of highly excited states, to work in the laboratory frame with good angular momentum and parity as allowed and forbidden transitions have strong and different selection rules, and to treat nuclei from light to superheavy ones. The projected shell model (PSM) [30,31], when updated with extended large configuration space [32,33], can serve as one of the candidate models for nuclear β and neutrino spectra. The PSM has been applied successfully on studies of nuclear levels [34,35] and weak-interaction processes [2,36–38] recently, with the help of some modern algorithms [39,40]. The exact angular-momentum-projection technique that is adopted by the PSM is also crucial for study of rare nuclear weak decays by other models [41,42]. We aim at developing the PSM further for description of nuclear total β and neutrino spectra step by step. In this work, we develop the PSM for calculation of the reduced one-body transition density (ROBTD) by the Pfaffian algorithm for nuclear β decays. On one hand, the ROBTD and level energy are indispensable nuclear inputs for the modern beta spectrum generator (BSG) code for highly precision theoretical description of the allowed one-to-one β spectrum [8]. On the other hand, the ROBTD is also one of the two indispensable ingredients for description of forbidden transitions. The latter has been accomplished and will be published elsewhere soon.

The paper is organized as follows. In Sec. II we introduce briefly the basic framework for β spectrum of allowed one-to-one transition and the BSG, in Sec. III the PSM for

ROBTD is presented. The β spectra for ^{162}Gd and ^{103}Ru are discussed in Sec. IV and we finally summarize our work in Sec. V.

II. GENERAL FORM OF β SPECTRUM FOR ALLOWED TRANSITION

Following Refs. [7,8], after introducing several corrections including atomic effects such as the screening and exchange processes, the analytical β spectrum of allowed one-to-one transitions with very high precision can be written as

$$\begin{aligned} \frac{dN(\omega)}{d\omega} = & \frac{G_V^2 V_{ud}^2}{2\pi^3} F_0(Z, \omega) p\omega(Q_{if} - \omega)^2 \\ & \times L_0(Z, \omega) C(Z, \omega) R(Q_{if}, \omega) X(Z, \omega) r(Z, \omega) \\ & \times U(Z, \omega) D(Z, \omega, \beta_2) R_N(Q_{if}, \omega) Q(Z, \omega) S(Z, \omega), \end{aligned} \quad (1)$$

where ω ($p = \sqrt{\omega^2 - 1}$) is the total energy (the momentum) of the electron in unit of $m_e c^2$ ($m_e c$), Z is the proton number of the daughter nucleus, and G_V the vector coupling strength. Q_{if} labels the available energy for leptons of the transition, i.e.,

$$Q_{if} = (\Delta M_{pd} + E_i - E_f)/m_e c^2, \quad (2)$$

where ΔM_{pd} denotes the nuclear-mass difference of parent and daughter nuclei and E_i (E_f) is the excitation energy of initial (final) state of parent (daughter) nucleus. It is noted that E_i is zero (has finite value) for the ground state (some isomer) of the decaying parent nucleus.

In Eq. (1) $F_0(Z, \omega)$ is the Fermi function reflecting the Coulomb distortion of electron radial wave function by the nuclear charge, representing the nucleus as a point particle. $p\omega(Q_{if} - \omega)^2$ is the phase space factor. These two terms dominate the β spectrum shape and are then the most crucial parts for β spectrum. It can be seen from Eqs. (1), (2) that nuclear level energies (E_i, E_f) are important for β spectrum as they affects the phase space factor. The following five terms are the main corrections to the β spectrum, in which $L_0(Z, \omega)$ is the correction factor to the analytical Fermi function so that the nuclear charge distribution is adopted as a uniformly charged sphere instead of a point nucleus. $C(Z, \omega)$ is the shape factor where radial wave function behavior and all nuclear-structure-sensitive information are included. The latter is concerned with four nuclear form factors relevant to allowed β decay (see Table I), which, following some approximations such as the impulse approximation, can be transformed into nuclear matrix elements of corresponding one-body operators, i.e. [7,8],

$$\begin{aligned} & \langle \Psi_{J_f}^{n_f} \| \hat{O}_\lambda \hat{\tau}^\pm \| \Psi_{J_i}^{n_i} \rangle \\ & = \hat{\lambda}^{-1} \sum_{\mu\nu} \langle \mu \| \hat{O}_\lambda \hat{\tau}^\pm \| \nu \rangle \langle \Psi_{J_f}^{n_f} \| [\hat{c}_\mu^\dagger \otimes \tilde{c}_\nu]^\lambda \| \Psi_{J_i}^{n_i} \rangle, \end{aligned} \quad (3)$$

where $\hat{\lambda} \equiv \sqrt{2\lambda + 1}$ with λ being the rank of operators, $|\Psi_{J_f}^{n_f}\rangle$ labels the nuclear many-body wave function for the n th eigenstate of angular momentum J , $\hat{\tau}^\pm$ is the isospin ladder operator for β^\pm decay so that μ and ν are

TABLE I. The four form factors for allowed Gamow-Teller decay. The first column shows the notation by Behrens and Bühring (BB) [44] and the second shows the evaluation of the form factor in the impulse approximation in cartesian coordinates, where M_N and R are the nucleon mass and nuclear radius, σ the Pauli matrix, $\beta = -\gamma_0$, and $\alpha = \gamma_5 \sigma$ with the Dirac γ matrices, g_A, g_M, g_P the coupling constant for axial, weak magnetism, and induced pseudoscalar currents, respectively, and the summation over nucleons and the isospin ladder operators are not shown for convenience. Refer to Refs. [7,8] for details.

Form factor (BB)	Matrix element (Impulse approximation)
$A F_{101}^{(0)}$	$\mp g_A \int \sigma$
$A F_{121}^{(0)}$	$\mp g_A \frac{3}{\sqrt{2}} \int \frac{(\sigma \cdot r) r - \frac{1}{3} \sigma \cdot r^2}{R^2} \pm g_P \frac{5\sqrt{2}}{(2M_N R)^2} \int \sigma$
$V F_{111}^{(0)}$	$-g_V \sqrt{\frac{3}{2}} \int \frac{\alpha \cdot r}{R} - (g_M - g_V) \frac{\sqrt{3}}{2M_N R} \int \sigma$
$A F_{110}^{(0)}$	$\pm g_A \sqrt{3} \int \gamma_5 \frac{ir}{R} \pm \frac{g_P \sqrt{3}}{(2M_N R)^2} (Q_{if} R \pm \frac{6}{5} \alpha Z) \int \sigma$

single-particle proton (neutron) and neutron (proton) states for β^- (β^+) decay. Here, we adopt the spherical harmonic oscillator basis so that $|\mu\rangle \equiv |n_\mu, l_\mu, j_\mu\rangle$ and \hat{c}^\dagger, \hat{c} are the corresponding single-particle creation and annihilation operators in the form of irreducible spherical tensor. The last term in Eq. (3) is the ROBTD which characterizes the many-nucleon properties of the initial (i) and final (f) nuclear states [43].

The $R(Q_{if}, \omega)$ term in Eq. (1) is the radiative correction corresponding to higher-order loop corrections for the interaction of the β particle and nucleus beyond the Fermi function [7,8]. The $X(Z, \omega)$ term is the correction for atomic exchange effect corresponding to the possibility of the β particle to be emitted into a bound state of the daughter atom by expelling the bound electron into the continuum. The $r(Z, \omega)$ term is the atomic mismatch correction that takes into account discrete processes such as shake-off and shake-up [7,8]. The last five terms in Eq. (1) are minor corrections that account for high-precision details of the β spectrum, where $U(Z, \omega)$ is for the diffused nuclear charge distribution near nuclear surface, $D(Z, \omega, \beta_2)$ for the small effect of nuclear deformation for charge distribution, $R_N(Q_{if}, \omega)$ for the effect of the recoil of a nucleus after β decay, $Q(Z, \omega)$ for the recoil Coulomb correction, and $S(Z, \omega)$ for the atomic screening correction that the β particle feels effective nuclear charge due to the screening of the orbiting electrons of the atom.

The analytical expressions of all the above corrections to allowed β spectrum have been studied in Ref. [7] in details, and a modern BSG code is developed in Ref. [8] to take into account all these corrections numerically for high-precision allowed β spectrum shapes, provided that some important nuclear-structure information such as the level energies and the ROBTD should be inputted. In this work we install, study, test, and employ the BSG code successfully and develop the PSM model for nuclear level energies and ROBTD successfully, then combine them for

the study of allowed one-to-one transition β spectrum shapes.

III. PROJECTED SHELL MODEL FOR LEVELS AND ROBTD

It is expected but not easy to develop a practical nuclear-structure model that can treat reasonably both allowed and forbidden transitions, having large model and configuration spaces for description of highly excited states, working in the laboratory frame with good angular momentum and parity for nuclear states as allowed and forbidden transitions have strong and different selection rules, and can treat even-even, odd-mass, and odd-odd nuclei from light to superheavy ones. We aim to accomplish this goal by further developing the PSM model extensively.

Due to the complexity of nuclear many-body problem, one of the practical solutions is to reduce the many-body to effective one-body problem by mean-field calculations in the intrinsic frame, then consider residual many-body correlations by beyond-mean-field methods and get the nuclear many-body wave functions in the laboratory frame. Following this philosophy, the PSM [30] starts from Nilsson+Bardeen-Cooper-Schrieffer (BCS) mean-field calculations (which can be generalized to elaborated ones for low-lying states [41,42]) and then adopts configuration mixing and angular-momentum projection (AMP) for the beyond mean-field part. The configuration spaces of the PSM are then

$$\begin{aligned}
ee : & \{ |\Phi\rangle, \hat{a}_{v_i}^\dagger \hat{a}_{v_j}^\dagger |\Phi\rangle, \hat{a}_{\pi_i}^\dagger \hat{a}_{\pi_j}^\dagger |\Phi\rangle, \hat{a}_{v_i}^\dagger \hat{a}_{v_j}^\dagger \hat{a}_{\pi_k}^\dagger \hat{a}_{\pi_l}^\dagger |\Phi\rangle, \\
& \hat{a}_{v_i}^\dagger \hat{a}_{v_j}^\dagger \hat{a}_{v_k}^\dagger \hat{a}_{v_l}^\dagger |\Phi\rangle, \hat{a}_{\pi_i}^\dagger \hat{a}_{\pi_j}^\dagger \hat{a}_{\pi_k}^\dagger \hat{a}_{\pi_l}^\dagger |\Phi\rangle, \dots \}, \\
ov : & \{ \hat{a}_{v_i}^\dagger |\Phi\rangle, \hat{a}_{v_i}^\dagger \hat{a}_{v_j}^\dagger \hat{a}_{v_k}^\dagger |\Phi\rangle, \hat{a}_{v_i}^\dagger \hat{a}_{\pi_j}^\dagger \hat{a}_{\pi_k}^\dagger |\Phi\rangle, \\
& \hat{a}_{v_i}^\dagger \hat{a}_{v_j}^\dagger \hat{a}_{v_k}^\dagger \hat{a}_{\pi_l}^\dagger \hat{a}_{\pi_m}^\dagger |\Phi\rangle, \dots \}, \\
o\pi : & \{ \hat{a}_{\pi_i}^\dagger |\Phi\rangle, \hat{a}_{\pi_i}^\dagger \hat{a}_{\pi_j}^\dagger \hat{a}_{\pi_k}^\dagger |\Phi\rangle, \hat{a}_{\pi_i}^\dagger \hat{a}_{v_j}^\dagger \hat{a}_{v_k}^\dagger |\Phi\rangle, \\
& \hat{a}_{\pi_i}^\dagger \hat{a}_{\pi_j}^\dagger \hat{a}_{\pi_k}^\dagger \hat{a}_{v_l}^\dagger \hat{a}_{v_m}^\dagger |\Phi\rangle, \dots \}, \\
oo : & \{ \hat{a}_{v_i}^\dagger \hat{a}_{\pi_j}^\dagger |\Phi\rangle, \hat{a}_{v_i}^\dagger \hat{a}_{v_j}^\dagger \hat{a}_{v_k}^\dagger \hat{a}_{\pi_l}^\dagger |\Phi\rangle, \hat{a}_{v_i}^\dagger \hat{a}_{\pi_j}^\dagger \hat{a}_{\pi_k}^\dagger \hat{a}_{\pi_l}^\dagger |\Phi\rangle, \\
& \hat{a}_{v_i}^\dagger \hat{a}_{v_j}^\dagger \hat{a}_{v_k}^\dagger \hat{a}_{\pi_l}^\dagger \hat{a}_{\pi_m}^\dagger \hat{a}_{\pi_n}^\dagger |\Phi\rangle, \dots \}, \tag{4}
\end{aligned}$$

for even-even (ee), odd-neutron (ov), odd-proton (o π), and odd-odd (oo) nuclei, respectively, where $|\Phi\rangle$ is the quasi-particle (qp) vacuum with associated intrinsic deformation and \hat{a}_v^\dagger (\hat{a}_π^\dagger) labels neutron (proton) qp creation operator. The large configuration spaces in Eq. (4) are developed in Refs. [32,33,36] recently and three or more major harmonic-oscillator shells can be adopted for model space. In this work, three major harmonic shells are taken in the model space, with $N = 3, 4, 5$ ($N = 2, 3, 4$) for neutrons (protons) of ^{103}Ru and ^{103}Rh , $N = 4, 5, 6$ ($N = 3, 4, 5$) for neutrons (protons) of ^{162}Gd and ^{162}Tb , and up to 4-qp (5-qp) configurations are adopted in the configuration spaces for even-mass (odd-mass) nuclei as shown in Eq. (4).

The many-body configurations in Eq. (4) cannot be adopted as the many-body basis as many symmetries are broken in the mean-field calculations in the intrinsic frame.

The projection technique can restore broken symmetries in the intrinsic frame and transform the configurations to projected basis in the laboratory frame [45]. For example, the broken rotational symmetry in deformed intrinsic mean fields can be restored by the AMP operator,

$$\hat{P}_{MK}^J = \frac{2J+1}{8\pi^2} \int d\Omega D_{MK}^{J*}(\Omega) \hat{R}(\Omega), \quad (5)$$

where \hat{R} and D_{MK}^J (with Euler angle Ω) [46] are the rotation operator and Wigner D function [40], respectively. The nuclear many-body wave function in the laboratory system can then be expressed in the projected basis,

$$|\Psi_{JM}^n\rangle = \sum_{K\kappa} f_{K\kappa}^{Jn} \hat{P}_{MK}^J |\Phi_\kappa\rangle, \quad (6)$$

where κ labels different qp configurations in Eq. (4), and the expansion coefficients $f_{K\kappa}^{Jn}$ can be obtained by solving the Hill-Wheeler-Griffin equation with appropriate many-body Hamiltonian, i.e.,

$$\sum_{K'\kappa'} [\mathcal{H}_{K\kappa K'\kappa'}^J - E_J^n \mathcal{N}_{K\kappa K'\kappa'}^J] f_{K'\kappa'}^{Jn} = 0, \quad (7)$$

where the projected matrix elements for the Hamiltonian and norm are

$$\mathcal{H}_{K\kappa K'\kappa'}^J = \langle \Phi_\kappa | \hat{H} \hat{P}_{K'\kappa'}^J | \Phi_{\kappa'} \rangle, \quad (8a)$$

$$\mathcal{N}_{K\kappa K'\kappa'}^J = \langle \Phi_\kappa | \hat{P}_{K'\kappa'}^J | \Phi_{\kappa'} \rangle. \quad (8b)$$

The level energies E_J^n can be obtained from Eq. (7) as well.

Conventionally transition strengths are calculated in the PSM by writing the transition operators (such as Gamow-Teller transition operator for β decay and electron-magnetic transition operators for spectroscopy) in the qp representation [30,36] instead of adopting the ROBTD. The ROBTD can be actually derived as

$$\begin{aligned} & \langle \Psi_{J_f}^{n_f} | [\hat{c}_\mu^\dagger \otimes \tilde{c}_\nu]^\lambda | \Psi_{J_i}^{n_i} \rangle \\ &= \sqrt{2J_f+1} \sum_{K\kappa K'\kappa'} f_{K\kappa}^{J_f n_f} f_{K'\kappa'}^{J_i n_i} \sum_{\rho} C_{J_i K - \rho \lambda \rho}^{J_f K} \\ & \times \frac{2J_i+1}{8\pi^2} \int d\Omega D_{K-\rho K'}^{J_i*}(\Omega) \sum_{m_\mu m_\nu} C_{j_\mu m_\mu j_\nu m_\nu}^{\lambda \rho} \\ & \times (-)^{j_\nu+m_\nu} \langle \Phi_\kappa | \hat{c}_{j_\mu m_\mu}^\dagger \hat{c}_{j_\nu - m_\nu} \hat{R}(\Omega) | \Phi_{\kappa'} \rangle, \end{aligned} \quad (9)$$

where C labels the Clebsch-Gordan coefficients, and the rotated matrix elements with mixed single-particle operators can be calculated by the modern Pfaffian algorithm [39,47] as

$$\begin{aligned} & \langle \Phi_\kappa | \hat{c}_{j_\mu m_\mu}^\dagger \hat{c}_{j_\nu - m_\nu} \hat{R}(\Omega) | \Phi_{\kappa'} \rangle \\ &= \langle \Phi^{(b)} | \hat{b}_1 \cdots \hat{b}_n \hat{c}_{j_\mu m_\mu}^\dagger \hat{c}_{j_\nu - m_\nu} \hat{R}(\Omega) \hat{a}_1^\dagger \cdots \hat{a}_{n'}^\dagger | \Phi^{(a)} \rangle \\ &= \text{Pf}(\mathbb{S}) \langle \Phi^{(b)} | \hat{R}(\Omega) | \Phi^{(a)} \rangle, \end{aligned} \quad (10)$$

where $|\Phi^{(a)}\rangle$ and $|\Phi^{(b)}\rangle$ label the qp vacua of parent and daughter nuclei with \hat{a}^\dagger and \hat{b} being the corresponding qp creation and annihilation operators, respectively. Here, Pf denotes the Pfaffian of some matrix, refer to Ref. [48] for the

detailed definition of Pfaffians and Ref. [49] for a numerical code for Pfaffians.

In Eq. (10) \mathbb{S} is a $(n+2+n') \times (n+2+n')$ skew-symmetric matrix, the corresponding matrix elements \mathbb{S}_{ij} can be obtained by

$$\begin{aligned} & \frac{\langle \Phi^{(b)} | \hat{b}_i \hat{b}_j \hat{R}(\Omega) | \Phi^{(a)} \rangle}{\langle \Phi^{(b)} | \hat{R}(\Omega) | \Phi^{(a)} \rangle} \equiv B_{ij}^b(\Omega) \quad (1 \leq i \leq n, 1 \leq j \leq n) \\ & \frac{\langle \Phi^{(b)} | \hat{b}_i \hat{c}_{j\mu}^\dagger \hat{R}(\Omega) | \Phi^{(a)} \rangle}{\langle \Phi^{(b)} | \hat{R}(\Omega) | \Phi^{(a)} \rangle} \quad (1 \leq i \leq n, j = n+1) \\ & \frac{\langle \Phi^{(b)} | \hat{b}_i \hat{c}_{j\nu - m_\nu} \hat{R}(\Omega) | \Phi^{(a)} \rangle}{\langle \Phi^{(b)} | \hat{R}(\Omega) | \Phi^{(a)} \rangle} \quad (1 \leq i \leq n, j = n+2) \\ & \frac{\langle \Phi^{(b)} | \hat{b}_i \hat{R}(\Omega) \hat{a}_j^\dagger | \Phi^{(a)} \rangle}{\langle \Phi^{(b)} | \hat{R}(\Omega) | \Phi^{(a)} \rangle} \equiv C_{ij}^{ba}(\Omega) \quad (1 \leq i \leq n, j > n+2) \\ & \frac{\langle \Phi^{(b)} | \hat{c}_{j\mu}^\dagger \hat{c}_{j\nu - m_\nu} \hat{R}(\Omega) | \Phi^{(a)} \rangle}{\langle \Phi^{(b)} | \hat{R}(\Omega) | \Phi^{(a)} \rangle} \quad (i = n+1, j = n+2) \\ & \frac{\langle \Phi^{(b)} | \hat{c}_{j\mu}^\dagger \hat{R}(\Omega) \hat{a}_j^\dagger | \Phi^{(a)} \rangle}{\langle \Phi^{(b)} | \hat{R}(\Omega) | \Phi^{(a)} \rangle} \quad (i = n+1, j > n+2) \\ & \frac{\langle \Phi^{(b)} | \hat{c}_{j\nu - m_\nu} \hat{R}(\Omega) \hat{a}_j^\dagger | \Phi^{(a)} \rangle}{\langle \Phi^{(b)} | \hat{R}(\Omega) | \Phi^{(a)} \rangle} \quad (i = n+2, j > n+2) \\ & \frac{\langle \Phi^{(b)} | \hat{R}(\Omega) \hat{a}_i^\dagger \hat{a}_j^\dagger | \Phi^{(a)} \rangle}{\langle \Phi^{(b)} | \hat{R}(\Omega) | \Phi^{(a)} \rangle} \equiv A_{ij}^a(\Omega) \quad (i > n+2, j > n+2) \end{aligned} \quad (11)$$

for $i < j$, and

$$\mathbb{S}_{ij} = -\mathbb{S}_{ji} \quad \text{for } (i > j). \quad (12)$$

In Eqs. (10), (11) the $\langle \Phi^{(b)} | \hat{R}(\Omega) | \Phi^{(a)} \rangle$, $A(\Omega)$, $B(\Omega)$, $C(\Omega)$ terms are the basic overlap and contractions [30,36] that have already been prepared in our PSM work for Gamow-Teller transitions (see Ref. [36] for details). The rest five basic contractions in Eq. (11) should be implemented numerically in the model. The expressions of them can be derived based on Hartree-Fock-Bogoliubov theory [45], the quantum theory of angular momentum [46], and some basic algorithms of AMP [30].

The ROBTD as shown in Eq. (9) can be used for study of allowed transition in β decays when restricting $\lambda = 0, 1$ and the indices μ, ν to keep the parity. Then, together with the level energies E_J^n in Eq. (7), they can provide important nuclear inputs for the BSG code for high-precision allowed β spectrum, which will be studied below. The expressions in Eqs. (9), (10), (11) have actually many more potential applications as well. On one hand, when restricting $\lambda = 0, 1, 2$ and the indices μ, ν to change the parity, the ROBTD serves as one of the two indispensable ingredients for description of first forbidden transitions in β decay. The PSM for first forbidden transition has been accomplished and will be published elsewhere soon. This indicates that the ROBTD developed in this work paves the way for theoretical description of the total β and neutrino spectra by the PSM where both allowed and forbidden transitions as well as the corresponding partial decay rates and $I(\%)$ can be calculated. On the other hand, the ROBTD make it possible to study interesting physics, such as the isovector spin monopole resonance, in a straightforward way. Besides, the expressions in Eqs. (9), (10), (11) can be revised straightforwardly to derive the reduced two-body transition density, which will be helpful for study of the nuclear matrix elements in neutrinoless double β decay, the g_A quenching problem by chiral two-body currents in single β decay [41,50–52], etc.

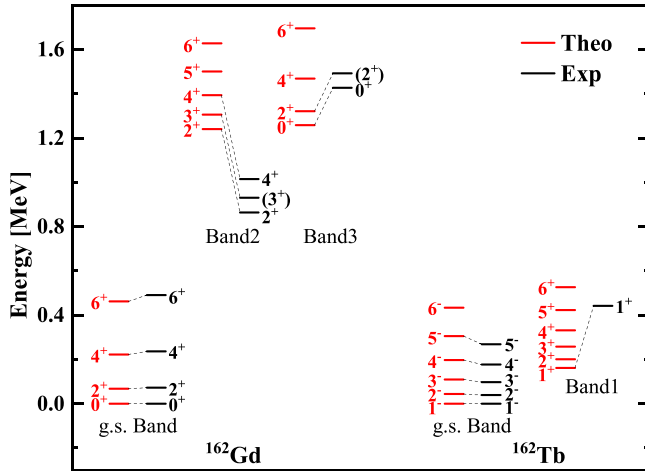


FIG. 2. The calculated levels, including the ground-state (g.s.) band and other side bands, of the parent nucleus ^{162}Gd and daughter nucleus ^{162}Tb , as compared with available data [53].

IV. RESULTS AND DISCUSSIONS

The level energies and ROBTd from the PSM calculations can be inputted to the BSG code to study their effects on the high-precision allowed β spectrum shape. Here, we take the transition from ^{162}Gd to ^{162}Tb as the first example from even-even to odd-odd nuclei, and the transition from ^{103}Ru to ^{103}Rh as the first example for odd-mass nuclei. These examples are adopted as one single allowed transition dominates the corresponding feeding intensity $I(\%)$ and therefore plays the most important role in the total spectrum for them. Except for the phase space factor and the shape factor $C(Z, \omega)$, the other corrections in Eq. (1) are all open with their parameters keeping to be the default values in the BSG code [8]. The coupling constants are adopted as their default values as $g_A = 1.0$, $g_M = 4.706$, and $g_P = 0$ [7,8], where g_A is different from its bare value due to the quenching effect [41,50–52].

Figure 2 shows the low-lying states, including the ground-state (g.s.) band and other side bands, of parent nucleus ^{162}Gd and daughter nucleus ^{162}Tb calculated by the PSM as compared with the data [53]. It is seen that the spin and parity of g.s. for both nuclei can be reproduced well and the structures of all bands are described reasonably, while some discrepancies exist for the band-head energies of side bands. The 0^+ g.s. of ^{162}Gd can decay to a 1^+ state of ^{162}Tb by allowed transition while other relevant transitions are all forbidden. This allowed transition dominates the β -decay feeding intensity of ^{162}Gd with $I(\%) = 95.5$, due to the strong transition strength with small $\log ft = 4.46$, which is reproduced reasonably by our PSM calculations as seen from Table II. These facts indicate that the nuclear many-body wave functions of both nuclei are described reasonably by the PSM, and the ROBTd calculated by the PSM should be appropriate.

With the ROBTd from PSM and the experimental level energies (442.1 keV) as inputs, the high-precision β spectrum for such a strong allowed transition is calculated by

TABLE II. The calculated $\log ft$ values for allowed transitions in the context, as compared with the corresponding data [53], see text for details.

Parent	$J_i^{\pi_i}$	Daughter	$J_f^{\pi_f}$	$\log ft_{(\text{Exp})}$	$\log ft_{(\text{PSM})}$
^{162}Gd	0^+	^{162}Tb	1^+	4.46	4.10
^{103}Ru	$3/2^+$	^{103}Rh	$5/2^+$	5.72	5.74

the BSG code, which is shown in Fig. 3 (blue dashed). When no external input for ROBTd of advanced many-body method is given, the BSG code has to evaluate nuclear matrix elements for form factors in Table I in an extreme simple single-particle (ESP) manner [8]. In the ESP case, the nuclear many-body wave function is approximated by a single-particle state closest to the neutron or proton Fermi surface for the final nucleon in a filling scheme. The picture is easy to understand for odd-mass nuclei, while for even-even and odd-odd nuclei the single-particle state of the last-filling nucleon is constructed using a spectator nucleon to obtain the correct angular momentum coupling. The analytical expression of nuclear matrix elements for even-mass and odd-mass nuclei can be obtained readily in the ESP case (see the Appendix of Ref. [8] for details). The ESP case corresponds to a pure single-particle manner neglecting many-nucleon correlations such as collective degrees of freedom and/or configuration mixing. Therefore the ESP evaluation may be a good approximation for very low-lying states of light and medium-heavy odd-mass nuclei, while its validity for other cases such as even-mass nuclei, heavy nuclei, transitions from isomers, transitions to excited states, etc., should be tested carefully by the elaborate many-body method for the nuclear matrix elements. When adopting the ESP evaluation [the spherical Woods-Saxon (WS) potential is adopted to avoid breaking the rotational symmetry] and the experimental level energies as inputs, the β spectrum for

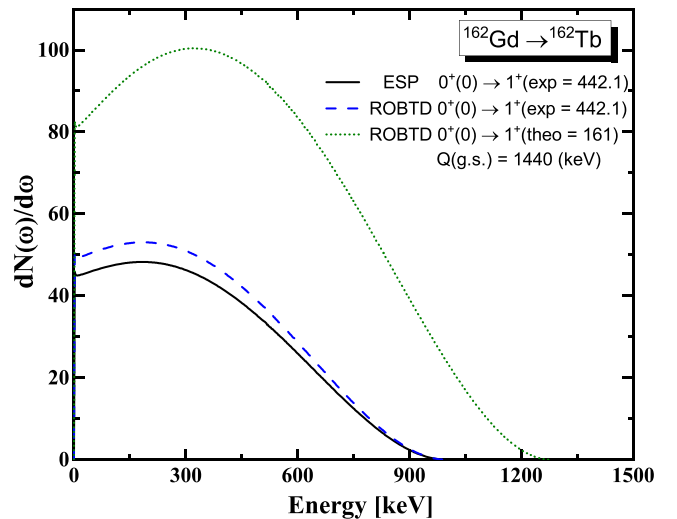


FIG. 3. The β spectrum for allowed $0^+ \rightarrow 1^+$ transition from ^{162}Gd to ^{162}Tb by the BSG code with different nuclear-structure inputs. See the text for details.

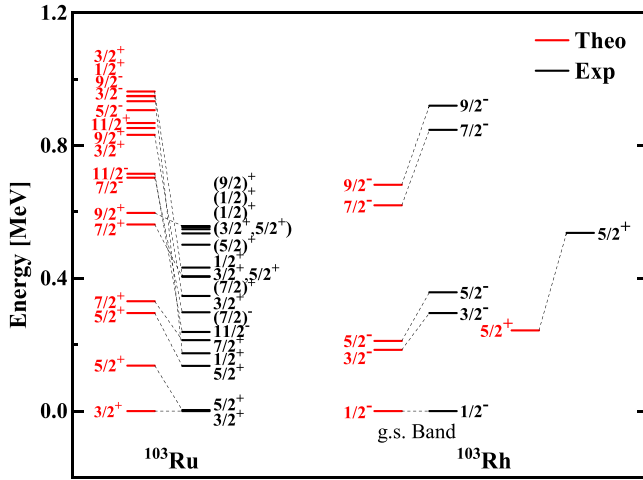


FIG. 4. The same as Fig. 2 but for the decay of ^{103}Ru to ^{103}Rh .

the allowed transition is shown in Fig. 3 by black solid line. It is seen that many-nucleon correlations in the ROBTD of PSM are important and turn out to increase the β spectrum by about 10%. Actually the 0^+ g.s. of ^{162}Gd is found to have collective qp vacuum as the main configuration and small mixing with a neutron 4-qp configuration, and the 1^+ state of ^{162}Tb has 2-qp $\nu 5/2^- [523] \otimes \pi 7/2^- [523]$ as the main configuration and about 8% mixing with some 4-qp configurations.

When the calculated level energies (161 keV) from the PSM are adopted as inputs, the corresponding β spectrum is shown in Fig. 3 by green dotted line. As the calculated 1^+ state of ^{162}Tb is lowered than the experimental level energy as shown in Fig. 2, the available energy for leptons of the transition, Q_{if} , is exaggerated, which increases the phase space factor as seen from Eqs. (1), (2) and accordingly the β spectrum since the phase space factor and Fermi function dominate the β spectrum shape. Although it is straightforward to see this conclusion, one should pay attention when nuclear-structure model calculations (for ROBTD and level energies, etc.) are indispensable for predicting β and neutrino spectra of exotic nuclei with very limited experimental data to solve problems such as the reactor antineutrino anomaly by for example the summation method in Ref. [24].

We finally report briefly the results for odd-mass nuclei. Figure 4 represents the calculated level energies for low-lying states of parent ^{103}Ru and daughter ^{103}Rh nuclei. It is seen that the spin and parity of g.s. for both odd-mass nuclei are reproduced successfully. Besides, the structure of the g.s. band of ^{103}Rh is described reasonably, including the signature-splitting behavior. The $3/2^+$ g.s. of ^{103}Ru can decay to a $5/2^+$ state of ^{103}Rh by allowed transition which dominates the β -decay feeding intensity with $I(\%) = 92.0$. The $\log ft$ of such a strong transition is well reproduced by the PSM calculations as seen from Table II. The β spectrum for such a allowed transition with different inputs, i.e., ROBTD by PSM or ESP, level energies of experimental data or PSM, is shown in Fig. 5. It is seen that when experimental level energies are adopted, the ROBTD from PSM tends to increase the spectrum by ESP

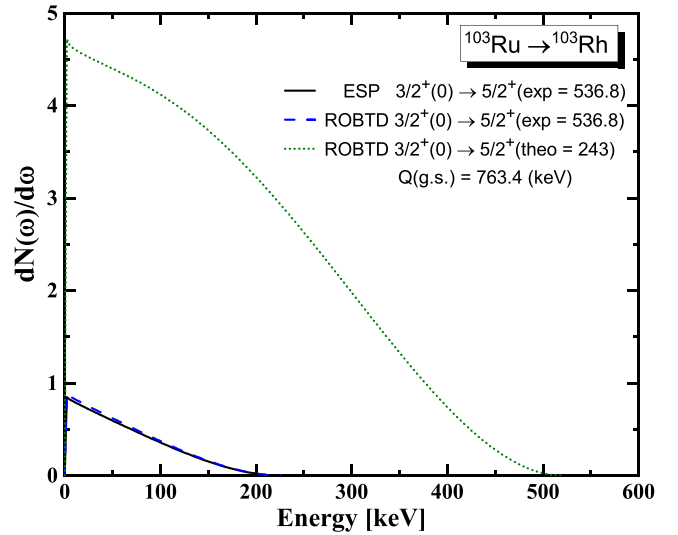


FIG. 5. The same as Fig. 3 but for the decay of ^{103}Ru to ^{103}Rh . See the text for details.

by about 5%, indicating that the single-particle approximation of the ESP may be more appropriate for odd-mass nuclei. The difference in β spectrum by the ROBTD and the ESP should come from nuclear many-nucleon correlations as well. The $3/2^+$ g.s. of ^{103}Ru is found to have 1-qp $\nu 3/2^+ [411]$ as the main configuration and 13% mixing with other 1-qp and 3-qp configurations, and the $5/2^+$ state of ^{103}Rh has 1-qp $\pi 5/2^+ [422]$ as the main configuration and 38% mixing with many 1-qp and 3-qp configurations. When the calculated level energies by the PSM are adopted as inputs, the corresponding β spectrum is shown to increase greatly due to the small β -decay Q value $Q_{\beta}(\text{g.s.}) = 763.4$ keV. It is worth mentioning that all the corrections in Eq. (1) are expected to contribute several percentage to the β spectrum where only purely the phase space factor and Fermi function are considered, when adopting the ESP approximation (see the Fig. 5 of Ref. [8] for example).

It is helpful to illustrate the effects of each of the various corrections in the β spectra when the ROBTD from complicated many-body calculations by the PSM is adopted. Figure 6 shows the ratio between the calculations where each correction in Eq. (1) is further taken into account based on the simple case where only the phase space $p\omega(Q_{if} - \omega)^2$ and Fermi function $F_0(Z, \omega)$ are considered, and the latter simple case. Corrections with the relative ratio less than 0.01 are neglected. It is seen that the Fermi-function correction L_0 and the radiative correction R (the atomic screening correction S) tend to provide positive (negative) relatively large effect, the shape factor C provides relatively small effect, the atomic exchange correction X , and the atomic mismatch correction r tend to affect the two sides of the β spectra, for the decays of ^{162}Gd and ^{103}Ru considered here.

Besides, it is interesting to study the effects of many-body correlations to the form factor ratio, since if only $^A F_{101}^{(0)}$ is taken in the impulse form, the shape factor should be independent of the electron energy. The following definitions for the form

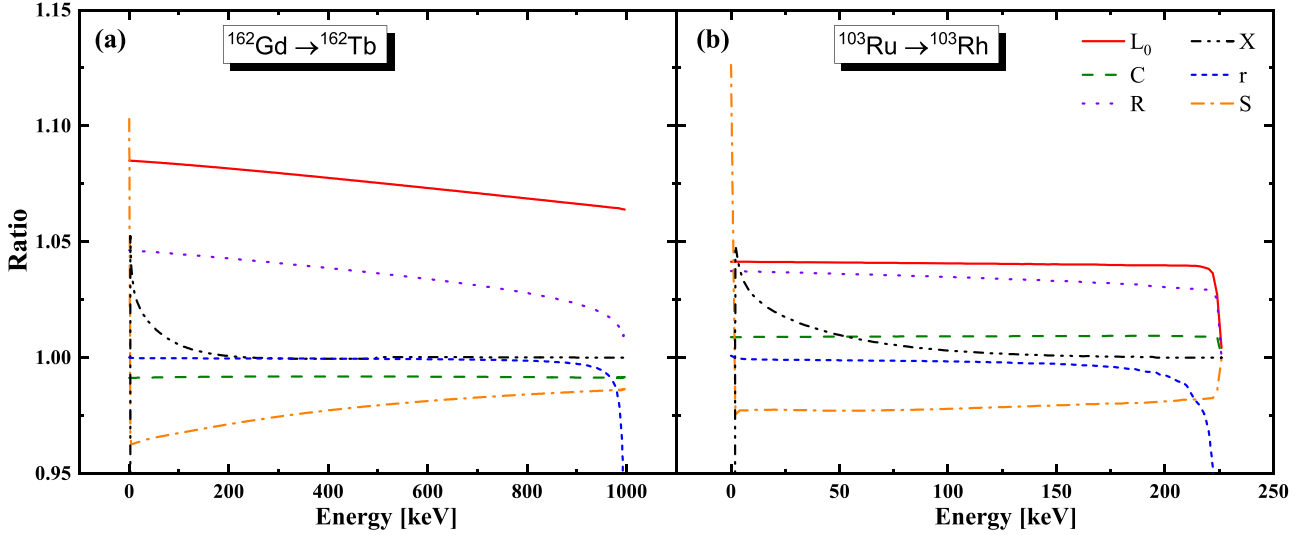


FIG. 6. The ratio between the consideration of each correction and the simple case where only the phase space and Fermi function are considered, as shown in Eq. (1). The ROBTd from the PSM is adopted, see the text for details.

factor ratio:

$$\frac{b}{Ac} = \frac{1}{g_A} \left[(g_M - g_V) - M_N R \sqrt{\frac{2}{3}} \frac{V F_{111}^{(0)}}{A F_{101}^{(0)}} \right], \quad (13a)$$

$$\frac{d}{Ac} = M_N R \frac{2}{\sqrt{3}} \frac{A F_{110}^{(0)}}{A F_{101}^{(0)}}, \quad (13b)$$

$$\Lambda = \frac{A F_{121}^{(0)}}{A F_{101}^{(0)}}, \quad (13c)$$

as in Ref. [8] is adopted with M_N being the nucleon mass, where it is noted that the definition of b looks different from that in Ref. [7]. The calculated values by the ESP and the ROBTd are shown in Table III, from which it is seen that the many-body correlations may be important as in many cases the results of the ROBTd deviate from the ones of ESP.

V. SUMMARY AND OUTLOOK

We aim to develop a shell-model method based on angular-momentum-projection techniques, for description of nuclear total β spectrum and neutrino spectrum, where both allowed and forbidden transitions can be treated, both large model space and configuration space are adopted for highly excited

TABLE III. The form factor ratio for the allowed transitions of Table II calculated by the ESP with WS potential and the ROBTd from the PSM.

Transition	Form factor ratio	ESP _{WS}	ROBTd
$^{162}\text{Gd} \rightarrow ^{162}\text{Tb}$	b/Ac	—	5.086
	d/Ac	—	5.102
	Λ	—	0.317
$^{103}\text{Ru} \rightarrow ^{103}\text{Rh}$	b/Ac	4.206	3.388
	d/Ac	-4.824	5.322
	Λ	0.349	0.367

states, the derived nuclear states are in the laboratory frame with good spin and parity, and that even-even, odd-odd, and odd-mass nuclei from light to superheavy ones can be described. As the first step, we developed our projected shell model (PSM) for calculating the reduced one-body transition density (ROBTd) for nuclear β decay (and also electron capture), by giving the analytical expression of the corresponding ROBTd with the Pfaffian algorithm. For the first application of our work, the calculated level energies and ROBTd from the PSM are inputted to the beta spectrum generator (BSG) code to study the high precision β spectrum of allowed transitions for even-mass case of $^{162}\text{Gd} \rightarrow ^{162}\text{Tb}$ and odd-mass case of $^{103}\text{Ru} \rightarrow ^{103}\text{Rh}$. When experimental level energies are adopted, the calculated β spectrum by ROBTd of the PSM where nuclear many-body correlations are treated reasonably, deviates from the β spectrum by the extreme simple-particle evaluation of the BSG by up to 10%. Besides, the calculated β spectrum shows sensitive dependence on the calculated level energies from nuclear models.

The next application of our work would be the description of first forbidden transitions in β decay, which is accomplished and will be published elsewhere soon. Then, it is possible to describe the total nuclear β and neutrino spectra by the PSM since both allowed and forbidden transitions as well as the corresponding partial decay rates and feeding intensity can be calculated theoretically.

Many more potential applications are also planned as near-future works, such as the isovector spin monopole resonance, etc., as well as deriving the reduced two-body transition density and then studying the nuclear matrix elements in neutrinoless double β decay, the g_A quenching problem by chiral two-body currents in single β decay, etc.

ACKNOWLEDGMENTS

L.J.W. would like to thank X. L. Huang and J. L. Liu for motivating the studies of nuclear β and neutrino spectra. This work is supported by the Fundamental Research Funds

for the Central Universities (Grant No. SWU-KT22050), by the National Natural Science Foundation of China (Grant No.

12275225), and partially supported by the Key Laboratory of Nuclear Data (China Institute of Atomic Energy).

-
- [1] H. Schatz, S. Gupta, P. Möller, M. Beard, E. F. Brown, A. T. Deibel, L. R. Gasques, W. R. Hix, L. Keek, R. Lau, A. W. Steiner, and M. Wiescher, Strong neutrino cooling by cycles of electron capture and β^- decay in neutron star crusts, *Nature (London)* **505**, 62 (2014).
- [2] L.-J. Wang, L. Tan, Z. Li, G. W. Misch, and Y. Sun, Urca cooling in neutron star crusts and oceans: Effects of nuclear excitations, *Phys. Rev. Lett.* **127**, 172702 (2021).
- [3] K. Langanke and G. Martínez-Pinedo, Nuclear weak-interaction processes in stars, *Rev. Mod. Phys.* **75**, 819 (2003).
- [4] J. J. Cowan, C. Sneden, J. E. Lawler, A. Aprahamian, M. Wiescher, K. Langanke, G. Martínez-Pinedo, and F.-K. Thielemann, Origin of the heaviest elements: The rapid neutron-capture process, *Rev. Mod. Phys.* **93**, 015002 (2021).
- [5] H. Schatz, A. Aprahamian, J. Görres, M. Wiescher, T. Rauscher, J. Rembges, F.-K. Thielemann, B. Pfeiffer, P. Möller, K.-L. Kratz, H. Herndl, B. Brown, and H. Rebel, rp-process nucleosynthesis at extreme temperature and density conditions, *Phys. Rep.* **294**, 167 (1998).
- [6] X. Mougeot, Reliability of usual assumptions in the calculation of β and ν spectra, *Phys. Rev. C* **91**, 055504 (2015).
- [7] L. Hayen, N. Severijns, K. Bodek, D. Rozpedzik, and X. Mougeot, High precision analytical description of the allowed β spectrum shape, *Rev. Mod. Phys.* **90**, 015008 (2018).
- [8] L. Hayen and N. Severijns, Beta spectrum generator: High precision allowed β spectrum shapes, *Comput. Phys. Commun.* **240**, 152 (2019).
- [9] A. Kumar, P. C. Srivastava, J. Kostensalo, and J. Suhonen, Second-forbidden nonunique β^- decays of ^{24}Na and ^{36}Cl assessed by the nuclear shell model, *Phys. Rev. C* **101**, 064304 (2020).
- [10] J. C. Hardy and I. S. Towner, Superallowed $0^+ \rightarrow 0^+$ nuclear β decays: 2014 critical survey, with precise results for V_{ud} and CKM unitarity, *Phys. Rev. C* **91**, 025501 (2015).
- [11] M. Bardies and J. F. Chatal, Absorbed doses for internal radiotherapy from 22 beta-emitting radionuclides: Beta dosimetry of small spheres, *Phys. Med. Biol.* **39**, 961 (1994).
- [12] G. Mention, M. Fechner, T. Lasserre, T. A. Mueller, D. Lhuillier, M. Cribier, and A. Letourneau, Reactor antineutrino anomaly, *Phys. Rev. D* **83**, 073006 (2011).
- [13] M. Fallot, S. Cormon, M. Estienne, A. Algora, V. M. Bui, A. Cucoanes, M. Elnimr, L. Giot, D. Jordan, J. Martino, A. Onillon, A. Porta, G. Pronost, A. Remoto, J. L. Taín, F. Yermia, and A.-A. Zakari-Issoufou, New antineutrino energy spectra predictions from the summation of beta decay branches of the fission products, *Phys. Rev. Lett.* **109**, 202504 (2012).
- [14] N. Haag, A. Gütlein, M. Hofmann, L. Oberauer, W. Potzel, K. Schreckenbach, and F. M. Wagner, Experimental determination of the antineutrino spectrum of the fission products of ^{238}U , *Phys. Rev. Lett.* **112**, 122501 (2014).
- [15] A.-A. Zakari-Issoufou, M. Fallot, A. Porta *et al.* (IGISOL Collaboration), Total absorption spectroscopy study of ^{92}Rb decay: A major contributor to reactor antineutrino spectrum shape, *Phys. Rev. Lett.* **115**, 102503 (2015).
- [16] F. P. An, A. B. Balantekin, H. R. Band *et al.* (Daya Bay Collaboration), Measurement of the reactor antineutrino flux and spectrum at Daya Bay, *Phys. Rev. Lett.* **116**, 061801 (2016).
- [17] J. H. Choi, W. Q. Choi, Y. Choi *et al.* (RENO Collaboration), Observation of energy and baseline dependent reactor antineutrino disappearance in the RENO experiment, *Phys. Rev. Lett.* **116**, 211801 (2016).
- [18] B. C. Rasco, M. Wolińska Cichocka, A. Fijałkowska, K. P. Rykaczewski, M. Karny, R. K. Grzywacz, K. C. Goetz, C. J. Gross, D.W. Stracener, E. F. Zganjar, J. C. Batchelder, J. C. Blackmon, N. T. Brewer, S. Go, B. Heffron, T. King, J. T. Matta, K. Miernik, C. D. Nesaraja, S. V. Paulauskas *et al.*, Decays of the three top contributors to the reactor $\bar{\nu}_e$ high-energy spectrum, ^{92}Rb , $^{96\text{gs}}\text{Y}$, and ^{142}Cs , studied with total absorption spectroscopy, *Phys. Rev. Lett.* **117**, 092501 (2016).
- [19] F. P. An, A. B. Balantekin, H. R. Band *et al.* (Daya Bay Collaboration), Evolution of the reactor antineutrino flux and spectrum at Daya Bay, *Phys. Rev. Lett.* **118**, 251801 (2017).
- [20] A. Fijałkowska, M. Karny, K. P. Rykaczewski, B. C. Rasco, R. Grzywacz, C. J. Gross, M. Wolińska Cichocka, K. C. Goetz, D. W. Stracener, W. Bielewski, R. Goans, J. H. Hamilton, J. W. Johnson, C. Jost, M. Madurga, K. Miernik, D. Miller, S. W. Padgett, S. V. Paulauskas, A. V. Ramayya *et al.*, Impact of modular total absorption spectrometer measurements of β decay of fission products on the decay heat and reactor $\bar{\nu}_e$ flux calculation, *Phys. Rev. Lett.* **119**, 052503 (2017).
- [21] A. A. Sonzogni, E. A. McCutchan, and A. C. Hayes, Dissecting reactor antineutrino flux calculations, *Phys. Rev. Lett.* **119**, 112501 (2017).
- [22] A. C. Hayes, G. Jungman, E. A. McCutchan, A. A. Sonzogni, G. T. Garvey, and X. B. Wang, Analysis of the Daya Bay reactor antineutrino flux changes with fuel burnup, *Phys. Rev. Lett.* **120**, 022503 (2018).
- [23] V. Guadilla, A. Algora, J. L. Tain *et al.*, Large impact of the decay of niobium isomers on the reactor $\bar{\nu}_e$ summation calculations, *Phys. Rev. Lett.* **122**, 042502 (2019).
- [24] M. Estienne, M. Fallot, A. Algora, J. Briz-Monago, V. M. Bui, S. Cormon, W. Gellelty, L. Giot, V. Guadilla, D. Jordan, L. Le Meur, A. Porta, S. Rice, B. Rubio, J. L. Taín, E. Valencia, and A.-A. Zakari-Issoufou, Updated summation model: An improved agreement with the Daya Bay antineutrino fluxes, *Phys. Rev. Lett.* **123**, 022502 (2019).
- [25] S. Al Kharusi, G. Anton, I. Badhrees *et al.* (EXO-200 Collaboration), Measurement of the spectral shape of the β -decay of ^{137}Xe to the ground state of ^{137}Cs in exo-200 and comparison with theory, *Phys. Rev. Lett.* **124**, 232502 (2020).
- [26] F. P. An, M. Andriamirado, A. B. Balantekin *et al.* (Daya Bay Collaboration and PROSPECT Collaboration), Joint determination of reactor antineutrino spectra from ^{235}U and ^{239}Pu fission by Daya Bay and prospect, *Phys. Rev. Lett.* **128**, 081801 (2022).
- [27] H. Almazán, M. Andriamirado, A. B. Balantekin *et al.* (PROSPECT Collaboration and STEREO Collaboration), Joint measurement of the ^{235}U antineutrino spectrum by prospect and stereo, *Phys. Rev. Lett.* **128**, 081802 (2022).

- [28] J. Hardy, L. Carraz, B. Jonson, and P. Hansen, The essential decay of pandemonium: A demonstration of errors in complex beta-decay schemes, *Phys. Lett. B* **71**, 307 (1977).
- [29] P. Shuai, B. C. Rasco, K. P. Rykaczewski *et al.*, Determination of β -decay feeding patterns of ^{88}Rb and ^{88}Kr using the modular total absorption spectrometer at ORNL HRIBF, *Phys. Rev. C* **105**, 054312 (2022).
- [30] K. Hara and Y. Sun, Projected shell model and high-spin spectroscopy, *Int. J. Mod. Phys. E* **4**, 637 (1995).
- [31] Y. Sun and D. H. Feng, High spin spectroscopy with the projected shell model, *Phys. Rep.* **264**, 375 (1996).
- [32] L.-J. Wang, F.-Q. Chen, T. Mizusaki, M. Oi, and Y. Sun, Toward extremes of angular momentum: Application of the Pfaffian algorithm in realistic calculations, *Phys. Rev. C* **90**, 011303(R) (2014).
- [33] L.-J. Wang, Y. Sun, T. Mizusaki, M. Oi, and S. K. Ghorui, Reduction of collectivity at very high spins in ^{134}Nd : Expanding the projected-shell-model basis up to 10-quasiparticle states, *Phys. Rev. C* **93**, 034322 (2016).
- [34] L.-J. Wang, J. Dong, F.-Q. Chen, and Y. Sun, Projected shell model analysis of structural evolution and chaoticity in fast-rotating nuclei, *J. Phys. G: Nucl. Part. Phys.* **46**, 105102 (2019).
- [35] L.-J. Wang, F.-Q. Chen, and Y. Sun, Basis-dependent measures and analysis uncertainties in nuclear chaoticity, *Phys. Lett. B* **808**, 135676 (2020).
- [36] L.-J. Wang, Y. Sun, and S. K. Ghorui, Shell-model method for Gamow-Teller transitions in heavy deformed odd-mass nuclei, *Phys. Rev. C* **97**, 044302 (2018).
- [37] L. Tan, Y.-X. Liu, L.-J. Wang, Z. Li, and Y. Sun, A novel method for stellar electron-capture rates of excited nuclear states, *Phys. Lett. B* **805**, 135432 (2020).
- [38] L.-J. Wang, L. Tan, Z. Li, B. Gao, and Y. Sun, Description of ^{93}Nb stellar electron-capture rates by the projected shell model, *Phys. Rev. C* **104**, 064323 (2021).
- [39] Z.-R. Chen and L.-J. Wang, Pfaffian formulation for matrix elements of three-body operators in multiple quasiparticle configurations, *Phys. Rev. C* **105**, 034342 (2022).
- [40] B.-L. Wang, F. Gao, L.-J. Wang, and Y. Sun, Effective and efficient algorithm for the Wigner rotation matrix at high angular momenta, *Phys. Rev. C* **106**, 054320 (2022).
- [41] L.-J. Wang, J. Engel, and J. M. Yao, Quenching of nuclear matrix elements for $0\nu\beta\beta$ decay by chiral two-body currents, *Phys. Rev. C* **98**, 031301(R) (2018).
- [42] J. M. Yao, J. Engel, L. J. Wang, C. F. Jiao, and H. Hergert, Generator-coordinate reference states for spectra and $0\nu\beta\beta$ decay in the in-medium similarity renormalization group, *Phys. Rev. C* **98**, 054311 (2018).
- [43] J. Suhonen, *From Nucleons to Nucleus* (Springer-Verlag, Berlin, 2007).
- [44] H. Behrens and W. Bühring, *Electron Radial Wave Functions and Nuclear Beta-Decay* (Clarendon Press, Oxford, 1982).
- [45] P. Ring and P. Schuck, *The Nuclear Many-Body Problem* (Springer-Verlag, Berlin, 1980).
- [46] D. A. Varshalovich, A. N. Moskalev, and V. K. Khersonskii, *Quantum Theory of Angular Momentum* (World Scientific Singapore, 1988).
- [47] Q.-L. Hu, Z.-C. Gao, and Y. Chen, Matrix elements of one-body and two-body operators between arbitrary HFB multi-quasiparticle states, *Phys. Lett. B* **734**, 162 (2014).
- [48] T. Mizusaki, M. Oi, F.-Q. Chen, and Y. Sun, Grassmann integral and Balian-Brézin decomposition in Hartree-Fock-Bogoliubov matrix elements, *Phys. Lett. B* **725**, 175 (2013).
- [49] C. González-Ballester, L. M. Robledo, and G. F. Bertsch, Numeric and symbolic evaluation of the Pfaffian of general skew-symmetric matrices, *Comput. Phys. Commun.* **182**, 2213 (2011).
- [50] G. Martínez-Pinedo, A. Poves, E. Caurier, and A. P. Zuker, Effective g_A in the pf shell, *Phys. Rev. C* **53**, R2602 (1996).
- [51] J. Menéndez, D. Gazit, and A. Schwenk, Chiral two-body currents in nuclei: Gamow-Teller transitions and neutrinoless double-beta decay, *Phys. Rev. Lett.* **107**, 062501 (2011).
- [52] P. Gysbers, G. Hagen, J. D. Holt *et al.*, Discrepancy between experimental and theoretical β -decay rates resolved from first principles, *Nat. Phys.* **15**, 428 (2019).
- [53] <https://www.nndc.bnl.gov>.